

The high resolution video capture system on the alcator C-Mod tokamak

A. J. Allen, J. L. Terry, D. Garnier, and J. A. Stillerman
Plasma Fusion Center, MIT, Cambridge, Massachusetts 02139-4307

G. A. Wurden
Los Alamos National Laboratory, Los Alamos, New Mexico 87545

(Presented on 15 May 1996)

A new system for routine digitization of video images is presently operating on the Alcator C-Mod tokamak. The PC-based system features high resolution video capture, storage, and retrieval. The captured images are stored temporarily on the PC, but are eventually written to CD. Video is captured from one of five filtered RS-170 CCD cameras at 30 frames per second (fps) with 640×480 pixel resolution. In addition, the system can digitize the output from a filtered Kodak Ektapro EM Digital Camera which captures images at 1000 fps with 239×192 resolution. Present views of this set of cameras include a wide angle and a tangential view of the plasma, two high resolution views of gas puff capillaries embedded in the plasma facing components, and a view of ablating, high speed Li pellets. The system is being used to study (1) the structure and location of visible emissions (including MARFEs) from the main plasma and divertor, (2) asymmetries in gas puff plumes due to flows in the scrape-off layer (SOL), and (3) the tilt and cigar-shaped spatial structure of the Li pellet ablation cloud. © 1997 American Institute of Physics. [S0034-6748(97)65101-1]

I. INTRODUCTION

Currently, Alcator C-Mod utilizes up to five arrays of H_α detectors¹ to unfold visible plasma emission from brightness data.² These consist of ~ 250 chords and require determination of the view of each detector, as well as the absolute intensity calibration of the view of each array. With the introduction of CCD technology on C-Mod, however, a view with over 300 000 different chords is available from a single camera. Since there is only one view, only one calibration must be made. Using a wide angle lens, large emission regions can be observed, and if toroidal symmetry is assumed, these multichord images may be inverted, in principle, to yield 2D poloidal cross sections of emissivity. The use of CCD images also brings with it new problems to be solved. The large amount of data available puts greater demands on data handling, storage, and manipulation technology. A formal inversion of these images has not been accomplished in the present work because of outstanding issues involving computer memory limits, chord selection, and reflection. Nonetheless, many of the preliminaries are finished. The viewing geometry of the wide-angle and tangential views has been determined. This has allowed location (determination of R and Z) of emission phenomena that are assumed to be toroidally symmetric. From knowledge of R and Z , flux surface perimeters can be mapped onto the video frames to show their relation to the emission. In addition, the present system for automatic digitization and acquisition of video images is being used routinely to measure flow in the SOL from gas puff plumes,³ and to measure tilt and spatial structure in Li pellet ablation clouds.⁴

II. EQUIPMENT

The video capture, storage, and retrieval system currently in use on C-Mod has four basic components: the video cameras, a framegrabber board for capturing and routing the video, a PC that temporarily stores video frames, and a CD-

write device for permanent data storage. A schematic of this system is shown in Fig. 1. There are two types of cameras currently in use with the system. There are five 8-bit RS-170 CCD cameras that take video at 30 fps with 640×480 resolution. There is also a Kodak Ektapro digital camera that captures up to 1600 frames at 1000 fps with 239×192 resolution. The digital camera stores the frames internally, and has been programmed to play back at 30 fps so that desired frames can be captured manually. The video from the RS-170 cameras is captured automatically using a triggered gate.

The video is captured from one of the available cameras with a commercial, PC-based framegrabber board, the Mu-Tech M-Vision 1000.⁵ The board's PCI bus architecture and its ability to directly control the mother board allow real-time video capture directly into the PC's memory. This eliminates expensive framegrabber onboard memory. The number of frames that can be captured is limited only by the amount of PC RAM available. For Alcator C-Mod it is desirable to digitize at 30 fps for ~ 1.5 s, the duration of a typical C-Mod discharge. Thus, the PC is equipped with 32 Mb of RAM, which is sufficient for the ~ 15 Mb of video as well as the overhead needed for running the Windows applications. The video is captured reliably in real time at 30 fps with known synchronization, since the board has an external "start" trigger or "on" gate. In addition, software has been written which plays the video on the monitor in slow motion and replays it continuously after a plasma discharge. A fast video board is required for full speed playback of high resolution video. A large capacity hard drive is also helpful since the video is memory intensive even with some level of compression.

Ultimately, the video must be permanently stored on removable media. Currently, the most economical media are writeable CDs with a capacity of 650 Mb per disc. With some compression (5:1), one CD is capable of storing about 9000 frames of video, which is approximately what is generated in one week of running Alcator C-Mod.

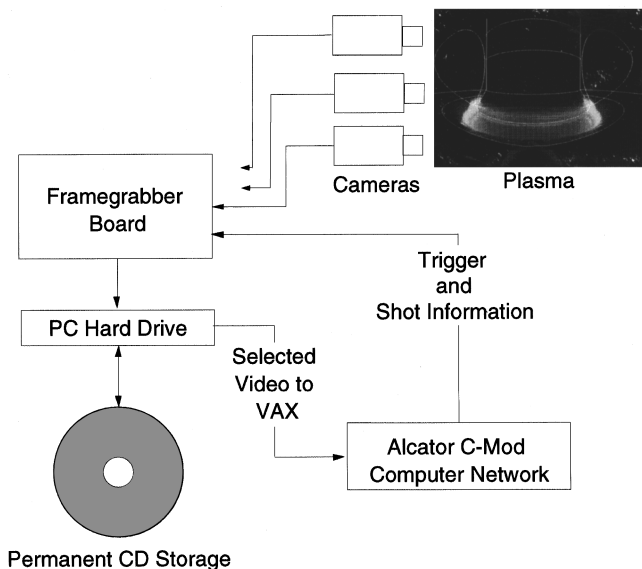


FIG. 1. Schematic of the new Alcator C-Mod video capture, storage, and retrieval system.

III. COMPRESSION AND FILE FORMATS

In uncompressed format (bitmaps), video of a 1.5 s plasma discharge requires about 15 Mb of storage space. A 650 Mb disc will hold only about 1800 uncompressed frames or 40 C-Mod shots. (This includes the unavoidable overhead on the CD of about 50 Mb.) Since the CDs take about 30 min to produce, some compression is desirable to increase the time between CD recordings. Presently available image compression algorithms are generally lossy. In particular, investigations of joint photographic experts group (JPEG), a popular single-frame compression format, reveal that a 5:1 compression ratio may be a reasonable compromise between intensity “distortion” and size compression. Typically, this compression yields average losses of less than 1 intensity unit (out of a full-scale value of 256), although some pixels had errors of 2–3 units, and a single pixel could have an error of as much as 10 units. Pixel intensity level and sharp intensity gradients had only minor effects on these values. It is difficult to see any visual difference between the compressed and uncompressed images, so this is certainly acceptable for “monitoring” purposes, however, it remains to be seen if the losses would significantly alter the results of an inversion. Another disadvantage of JPEG is that it operates only on individual frames, and therefore, yields no compression gain frame-to-frame. There are other formats that work on a sequence of frames and allow the frames to be played back as a movie. One example is the Windows .avi standard. It allows full 640×480 resolution and supports a variety of compression schemes and ratios, but is not lossless. Another promising full-motion scheme is multiframe GIF. It has the advantage of being a lossless process, but it appears to be limited to 3:2 compression. The popular motion picture experts group (MPEG) format was also investigated, but its maximum allowable resolution was quite limited (320×240 appears to be the upper functional limit).

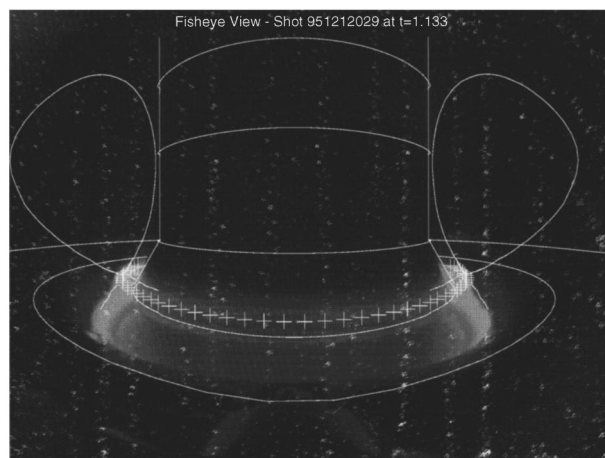


FIG. 2. Unfiltered, wide angle view of the discharge with predicted locations of various features on the vessel inner column and in the divertor region mapped onto the video frame. The perimeters of the last closed flux surface are also mapped at the toroidal angles where the emission appears to begin to curve back around the inner column. The rendered location of the x point is shown by the +’s.

IV. DETERMINATION OF THE VIEWING GEOMETRY

In order to extract quantitative information from the captured video, the geometry of the view with respect to the machine has to be determined. Once the viewing geometry is known, it is then possible to calculate the viewing chord of a given pixel. Knowledge of the pixel views is critical to the ultimate goal of unfolding the 2D poloidal emissivity from the view of the 3D scene.

In the absence of aberrations, the angle (with respect to the central ray) is preserved between object and image space. This allows calculation of the chordal view coordinates (relative to the plasma/vacuum vessel geometry) of any CCD pixel, given knowledge of: the pixel array geometry, the lens focal length, the position of the lens in the vacuum vessel, and the yaw, pitch, and roll of the camera. In the absence of exact knowledge of all these quantities or as a check of the quantities, one can calculate from object space to image space by using the known (vessel) coordinates of objects (e.g., ports, antennas, armor tiles) to predict the pixel positions of these objects in the image. This prediction can then be compared with the pixel positions that are actually observed in the image. This procedure has been carried out for two of the camera views on Alcator C-Mod. For the wide angle view shown in Fig. 2, significant corrections due to “barrel” image distortion by the lens were required to match the predicted image positions with those measured. After modeling these corrections, it was possible to reproduce the rendered positions of known and seen objects (e.g., the armor tiles on the inner cylinder and the location of one of the access ports). The predicted location for the inner cylinder, the midplane of the inner cylinder, and some of the divertor structures are shown as solid white lines in Fig. 2.

The equations and the modeled distortion corrections can be inverted to yield the required pixel views. This procedure amounts to rendering the 3D view onto the 2D CCD chip. With this ability, one can render structures in the view like flux surface perimeters whose geometry relative to the

machine is approximately known from C-Mod's flux surface reconstruction procedure EFIT.⁶ For example, the perimeter of the last closed flux surface (LCFS) is shown in Fig. 2 as it would appear in a plane perpendicular to the line of sight passing through its center.

V. USES OF VIDEO ON ALCATOR C-MOD

The captured video is currently being used to view emission "plumes"³ observed when gases (D_2 , He, CD_4 , N_2 , Ne) are puffed from capillary tubes embedded in the wall armor at various places around the machine. The strong spatial asymmetries seen in some plumes are being modeled to determine the bulk flow in the plasma scrape off layer.⁷ The video is also being used to investigate the size, shape and tilt angle of the cigar-shaped emission clouds of ablating lithium pellets. Tilt angle versus radius can be used to determine the plasma current density profile.⁴ The main focus of this work, however, is to model the visible emission features observed on Alcator C-Mod, as part of a preliminary investigation whose final goal is inversion of the measured 3D visible radiation to yield the 2D poloidal emissivity assuming toroidal symmetry.

A. Locating toroidally symmetric visible emission

With the geometry of a given view known, it is possible to determine the location of the visible emission in the plasma. Without a full-blown inversion, it is not possible to calculate the emissivities within the field of view. However, the R and Z values of toroidally symmetric emission seen in the view can be determined. Shown in Fig. 2 is the unfiltered emission from a typical discharge with a lower single null. Also shown are the perimeters of the LCFS as calculated by EFIT at the toroidal angles where the toroidally symmetric emission appears to curve back around the inner column. This determines the R and Z location of the emission. It can be seen in Fig. 2 that the emission is primarily outside the LCFS, in the SOL and in the private flux region.

B. Locating synchrotron radiation from runaway electrons

At densities below $\bar{n}_e \sim 5 \times 10^{19} \text{ m}^{-3}$ on Alcator C-Mod, the possibility exists for generating runaway (highly relativistic) electrons. The presence of these runaway electrons is detected by measuring the hard x-rays resulting from electron collisions with surrounding solid materials. During C-Mod's last campaign, there were several low density shots with some runaway population. Correlated with each of these shots was visible emission from well inside the LCFS that was observed by two of the CCD cameras. This emission is synchrotron radiation of the runaway electrons, generated as they move around the torus. As the electrons' velocity becomes a significant fraction of the speed of light, their emission is greatly collimated in the direction of travel. This collimation is shown quite clearly in the unfiltered wide angle view in Fig. 3. The emission is seen only on the left side of the torus where the electron flow is toward the camera. The fact that the emission is in the spectral range of the camera ($< 1.4 \mu\text{m}$) implies that the parallel electron energy of the

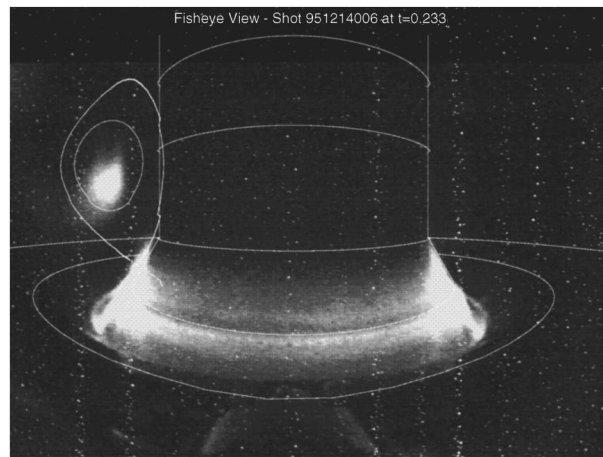


FIG. 3. Unfiltered, wide angle view with synchrotron radiation from runaway electrons seen on the left side of the vessel inner column. The perimeter of the LCFS and an inner flux surface are mapped at the toroidal angle where the field line tilt at the center of the observed emission is such that it points directly into the lens of the camera. Thus, the highly collimated synchrotron emission, which is aligned with the field lines, is seen. The majority of the image spot is thus seen at $Z < 0$. This is consistent with the local field line tilt and the viewing angles, since the camera is located below the midplane and looks horizontally into the machine.

runaways is $> 45 \text{ MeV}$ and the cone of emission is within $\pm 0.3^\circ$ of the electrons' velocity direction.⁸ Thus, the relatively large size of the emission image implies that the runaway electrons are present over a spatial region at least as big as the image seen in Fig. 3. An image of the synchrotron emission is also seen at the same time by a camera whose view is closer (than the wide angle view) and nearly tangential to the plasma column. This view is shown in Fig. 4 as seen through an H_α filter.

Using EFIT, flux surface perimeters can be mapped onto the views at toroidal angles where the field line tilt at the center of the observed emission is such that it points directly into the lens of the camera. Thus, the highly collimated synchrotron emission, which is aligned with the field lines, is seen. Flux surface perimeters mapped in this way can be found in Figs. 3 and 4. From these figures, it can be seen that the emission is asymmetric with respect to the plasma minor radius and poloidal angle. This is due to the field line pitch's relationship to the viewing angle. The camera in the wide angle view (Fig. 3) is located below the midplane looking horizontally, and the emission is seen at $Z < 0$. The camera in the tangential view (Fig. 4) is located above the midplane looking slightly down, and the emission is seen at $R < R_0$. Both of these emission locations are consistent with the field line tilt present in the discharge. (The toroidal magnetic field and plasma current are both in the clockwise direction as seen from above the tokamak.)

C. Fast fluctuations of visible emission

The Kodak digital camera has allowed study of visible emission phenomena on much shorter time scales (1 ms) than standard RS-170 CCD cameras (33 ms). This allows observation of phenomena that occur on faster time scales, such as impurity injections and disruptions.

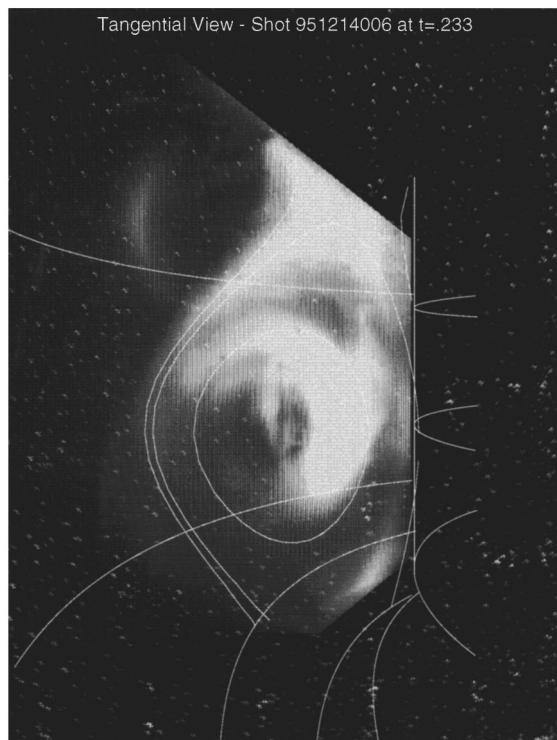


FIG. 4. Tangential view of the synchrotron radiation (filtered with a $\sim 50 \text{ \AA}$ bandpass at 6560 \AA) in the same discharge and at the same time as in Fig. 3. In this view, the vessel inner column is located at the right and the rf antenna can be seen at the left. Inner column and divertor features are mapped on the frame as solid white lines. The perimeter of an outer flux surface, the LCFS, and the same inner flux surface as shown in Fig. 3 are mapped at the toroidal location where the field line tilt points at the lens of the camera. The emission is seen at $R < R_0$. This is consistent with the local field line tilt and the viewing angles, since the camera is located above the midplane and is looking down slightly.

Typically, early in an Alcator C-Mod plasma discharge ($0 < t < 0.3 \text{ s}$), the plasma is limited on the inner wall. During this time, streamers of H_α (and CIII) light can be seen that fluctuate greatly between frames. Analyses of these frames have shown that $\sim 80\%$ of illuminated chords have brightnesses, I , that vary by $(\tilde{I}/\langle I \rangle) \geq 1$ when averaged over 30 ms, where \tilde{I} is the standard deviation of the brightnesses over the 30 ms, and $\langle I \rangle$ is average brightness over the interval. Also, 10%–20% of the chords have $(\tilde{I}/\langle I \rangle) \geq 0.25$, averaged

over the same interval. This shows that there is extensive emission fluctuation being averaged out by standard 30 fps CCD cameras early in the discharge.

VI. CONCLUSIONS

The new system for routine digitization of video images on Alcator C-Mod has been described. This system has made large quantities of high spatial resolution video easily available for study. The video is being used in a number of ways. Images of gas puffs are being used to measure the asymmetric flows in the SOL, and Li pellet ablation clouds are being used to measure field line tilt versus radius in order to determine the plasma current density profile. The R and Z values of toroidally symmetric visible emission have been determined, and flux surface perimeters have been mapped onto the video frames to show their relationship to emission. The synchrotron emission from runaway electrons has been analyzed, and a lower limit on the electron energy of $\sim 45 \text{ MeV}$ has been calculated. Also, an upper limit of $\sim 0.3^\circ$ for the size of the collimated emitting cone has been calculated. Finally, fluctuations of visible emission were investigated using the 1000 fps Kodak digital camera view. It was found that $\sim 80\%$ of illuminated chords have brightnesses, I , that varied by $(\tilde{I}/\langle I \rangle) \geq 1$ when averaged over 30 ms, where \tilde{I} is the standard deviation of brightnesses over the 30 ms, and $\langle I \rangle$ is average brightness over the interval. Also, 10%–20% of the chords have $(\tilde{I}/\langle I \rangle) \geq 0.25$, when averaged over the same interval.

ACKNOWLEDGMENTS

Work supported at MIT by DOE Contract No. DE-AC02-78ET51013 and at LANL by DOE Contract No. W-7405-ENG-36.

- ¹J. L. Terry, J. A. Snipes, and C. Kurz, *Rev. Sci. Instrum.* **66**, 555 (1995).
- ²C. Kurz, J. A. Snipes, J. L. Terry, B. LaBombard, B. Lipschultz, and G. M. McCracken, *Rev. Sci. Instrum.* **66**, 619 (1995).
- ³D. Jablonski *et al.*, *J. Nucl. Mater.* (to be published).
- ⁴D. Garnier, Ph.D. thesis, Massachusetts Institute of Technology Cambridge, MA, 1996.
- ⁵Framegrabber board made by the MuTech Corporation, Billerica, MA.
- ⁶L. L. Lau, H. St. John, R. D. Stambaugh, A. G. Kellman, and W. Pfeiffer, *Nucl. Fusion* **25**, 1611 (1985).
- ⁷D. Jablonski, Ph.D. thesis Massachusetts Institute of Technology Cambridge, MA 1996.
- ⁸J. D. Jackson, *Classical Electrodynamics* (Wiley, New York, 1962).